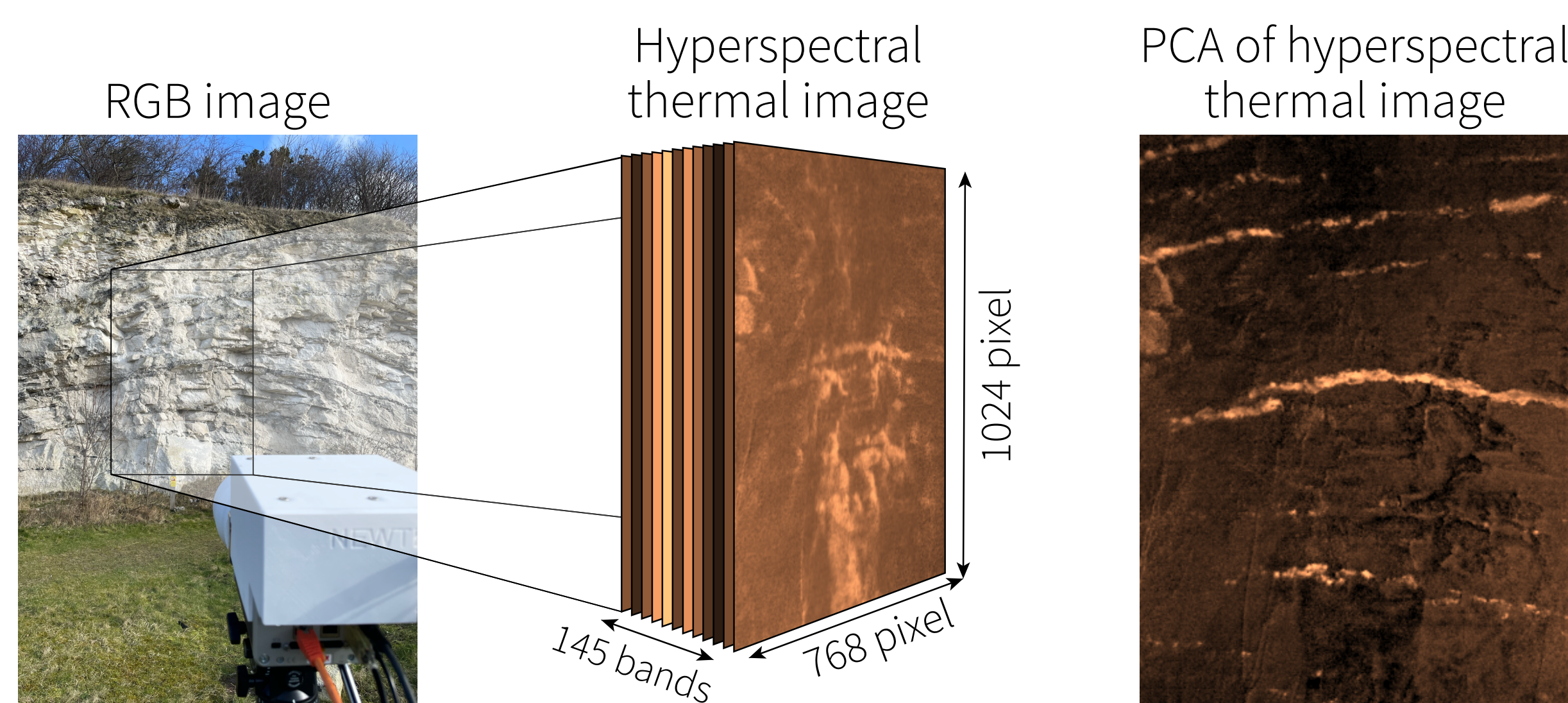


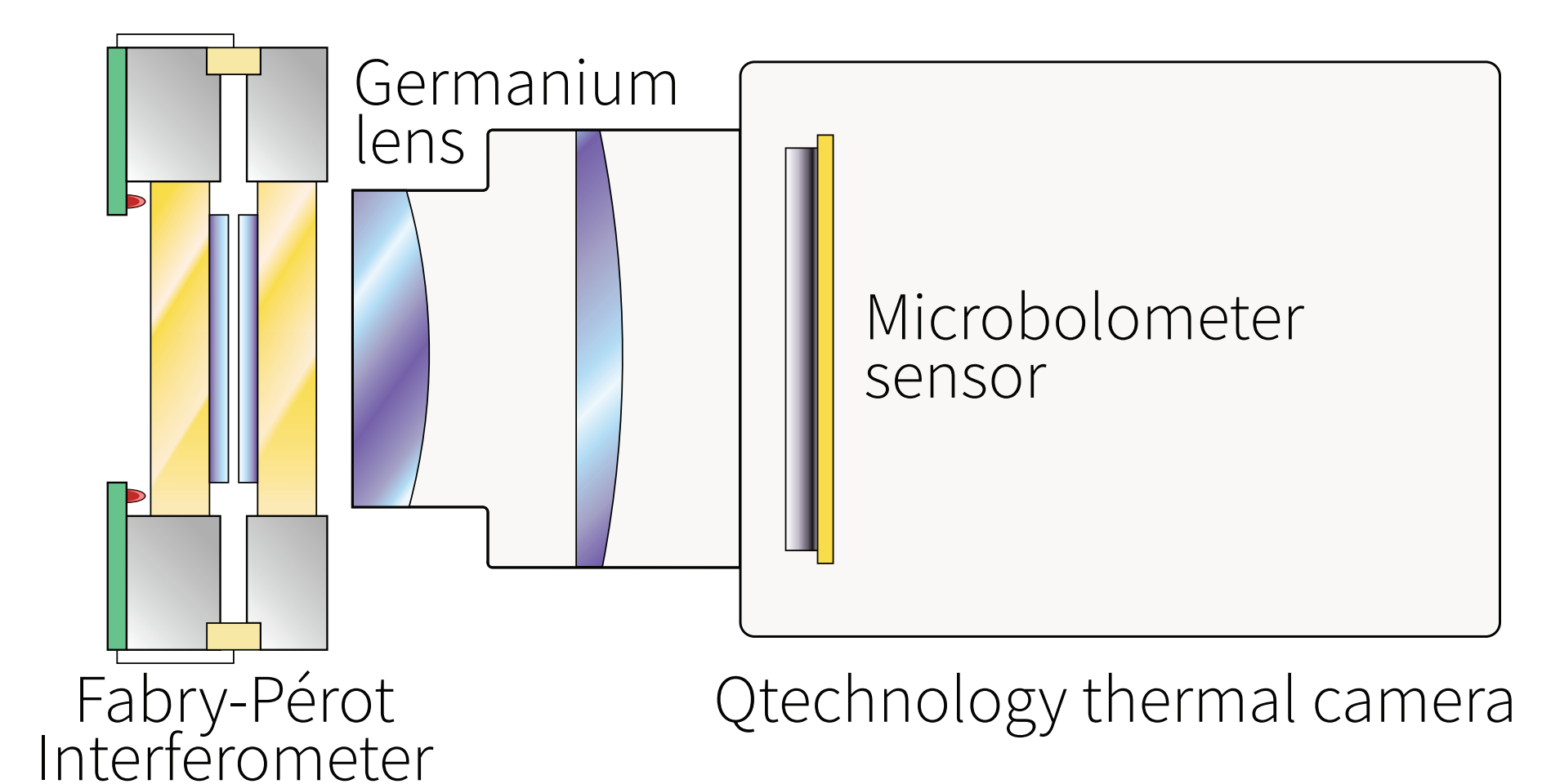
## 1 Introduction

Hyperspectral imaging in the longwave infrared (LWIR) domain can be used to measure spectral features of materials corresponding to the vibrational frequencies of its atomic bonds. This information can be used to determine what material(s) are being imaged. The selection of commercially available hyperspectral thermal imagers is scarce, expensive and many require cryogenic cooling. We here present a relatively inexpensive, spectral scanning, hyperspectral thermal camera (HSTC), capable of being brought to the field.



## 2 The camera

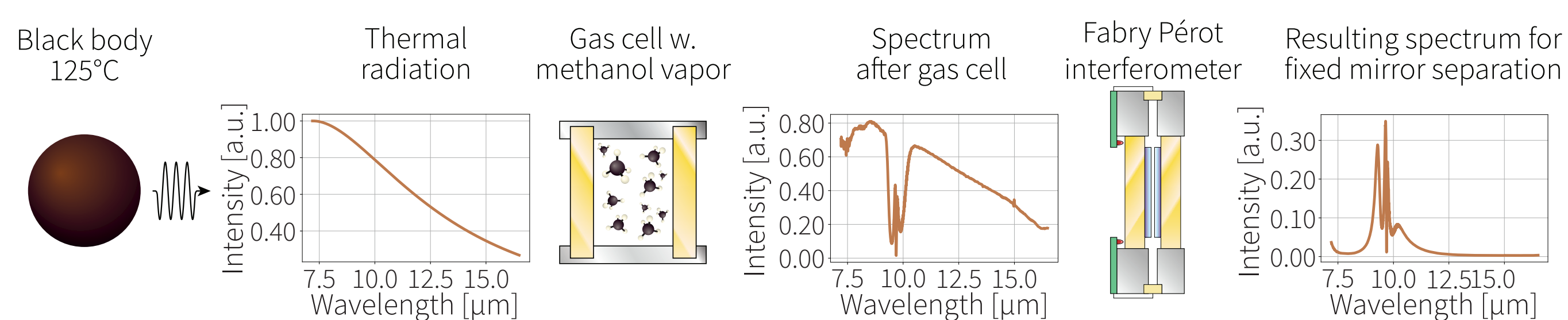
This hyperspectral thermal camera utilizes an uncooled microbolometer sensor capable of measuring thermal radiation with wavelengths ranging from **8 – 15 μm**. This range is split up into smaller parts by placing a scanning Fabry-Pérot interferometer (SFPI) in front of the camera. The SFPI acts as a variable bandpass filter where the mirror separation determines the distribution of wavelengths reaching the sensor. A hyperspectral image cube is formed by sweeping the mirror separation distance from  $\approx 3 - 12 \mu\text{m}$  and simultaneously acquiring  $\approx 145$  images with a spatial resolution is  $768 \times 1024$  pixels. A detailed description of the hyperspectral imaging system is given in [1].



## 3 Use cases

### Comparing hyperspectral thermal images and FTIR spectra

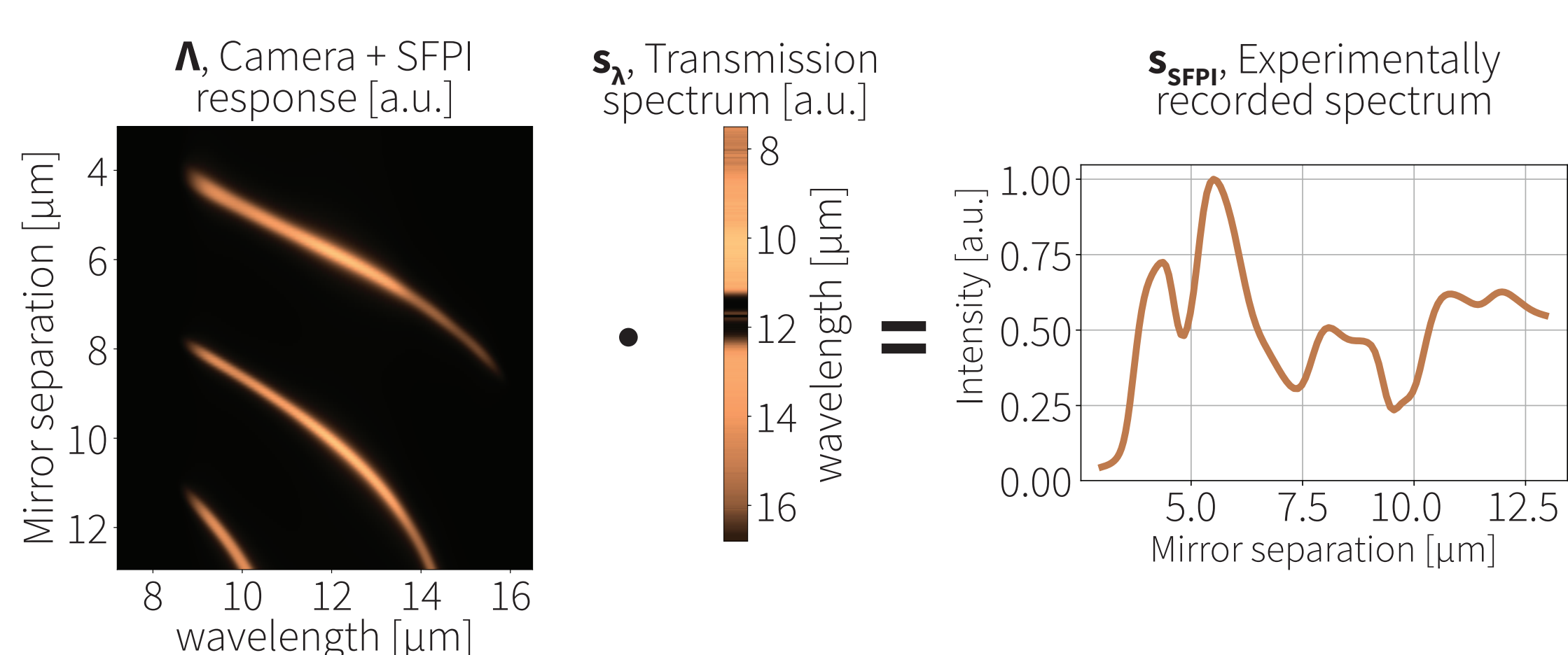
Many organic gases have spectral features in the LWIR region, and which can be recognized by the HSTC. Here we show how spectra of gaseous methanol recorded with HSTC can be compared to FTIR spectra.



The spectra recorded by the HSTC are given in terms of mirror separation and *not* wavelength. Linear algebra is used to describe the relationship between the wavelength dependent spectrum passing through the SFPI and the spectrum recorded by the HSTC. Firstly, the transmission through the SFPI is found using a transfer matrix method (TMM) at several mirror separations. This is combined with the spectral sensitivity of the camera and forms a matrix,  $\Lambda$ . The transmission spectrum of the gas is represented by the vector,  $s_\lambda$ . Finally, the SFPI spectrum,  $s_{\text{SFPI}}$ , can be readily found by:

$$\Lambda s_\lambda = s_{\text{SFPI}}$$

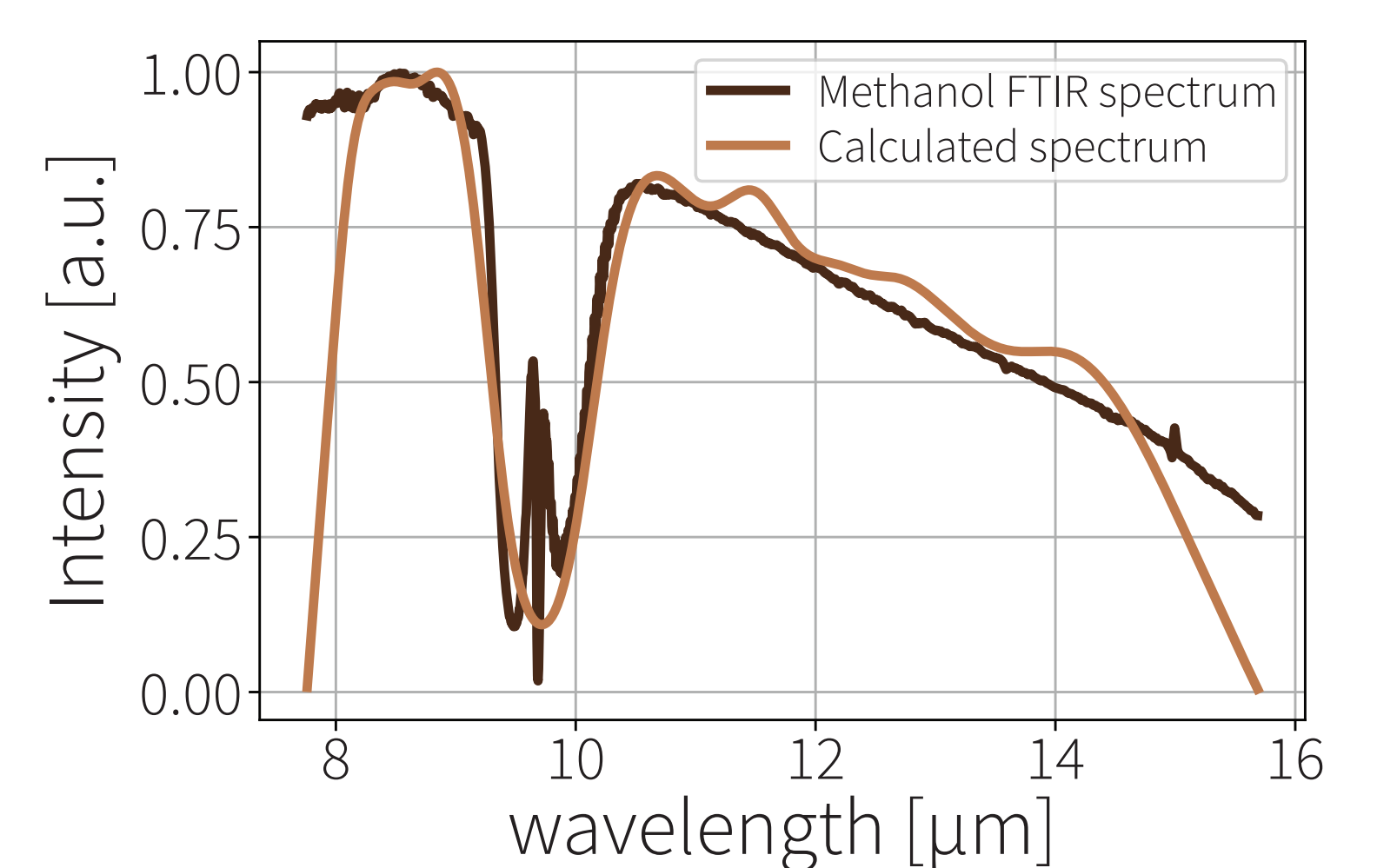
which can be represented graphically as:



Since the experimentally recorded spectra are in terms of mirror separation, it must be converted to the wavelength domain for comparison with FTIR. This is done by multiplying by  $\text{inv}(\Lambda)$  from the left. However, the matrix must be regularized by adding a matrix,  $M$ , representing the second derivative operator (finite difference).  $M$  has 2s along its diagonal, negative 1s above and below

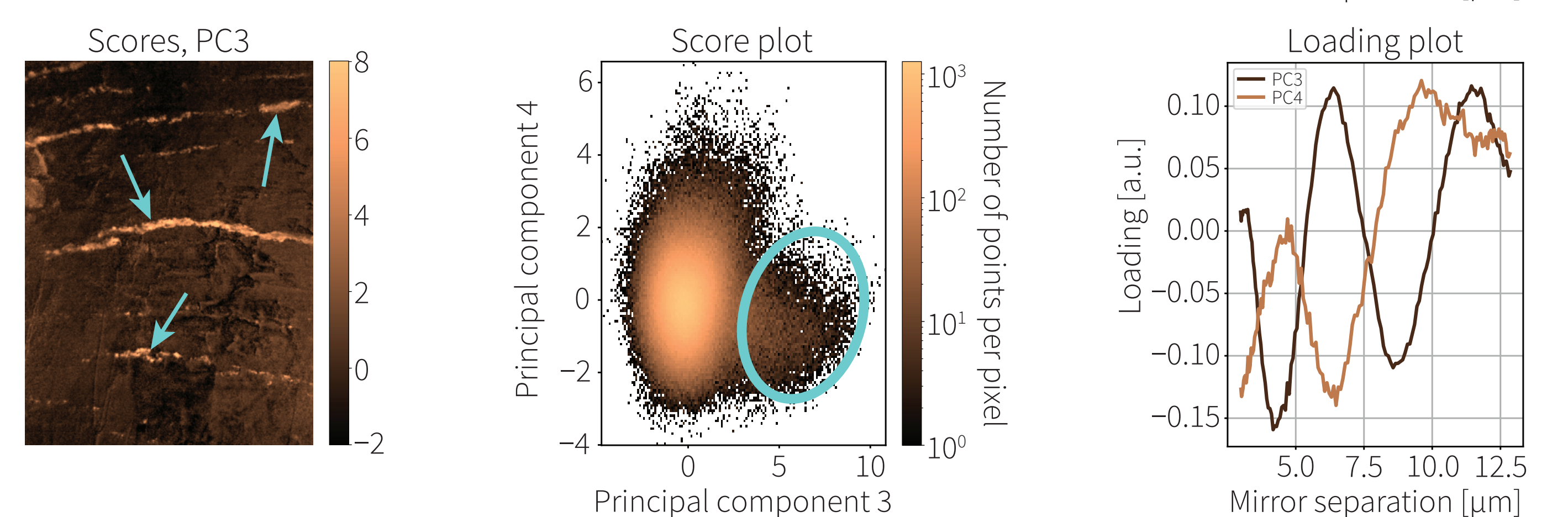
the diagonal, and 0s everywhere else.  $M$  is scaled by a factor,  $\alpha$ , before adding it to  $\Lambda$ . This form of regularization reduces oscillations in the resulting spectrum. Finally, the wavelength dependent transmission spectrum is calculated as

$$s_\lambda = \text{inv}(\Lambda^T \Lambda + \alpha M) \Lambda^T s_{\text{SFPI}}$$



### Detecting minerals

Another use case for the hyperspectral thermal camera is for distinguishing different types of minerals based on measured reflectance spectra. Here it is demonstrated how flint layers in a limestone cliff face is brought out using principal component analysis. The hyperspectral thermal image is captured at Boesdal limestone quarry.



## 4 Conclusions

A thermal camera combined with a scanning Fabry-Pérot interferometer is capable of capturing hyperspectral images. The spectra are recorded in terms of mirror separation distance and must be converted to wavelengths for comparison with literature. Several improvements are envisioned for the system, such as improved mirror control, and inclusion of RGB data (visual range).

